NORSAR

ROYAL NORWEGIAN COUNCIL FOR SCIENTIFIC AND INDUSTRIAL RESEARCH

Scientific Report No. 2-80/81

SEMIANNUAL TECHNICAL SUMMARY 1 October 1980—31 March 1981

By
Alf Kr. Nilsen (ed.)

Kjeller, June 1981

VI.9 Lithospheric Studies Based on the Principles of Holography

Concerning the possibility of using NORSAR short period data for wave field reconstruction procedures the main doubts were towards the gross undersampling of the wave field. Actually, the results obtained in the framework of random scattering and 'blocky' models (Berteussen et al, 1975; Aki et al, 1977) could not explain all the peculiarities of observed wave fields and therefore indicated a possibility of introducing the deterministic scattering model, assuming the pressence of 'strong' discrete inhomogeneities. To test NORSAR array 'holographic' feasibilities, an ultrasonic modelling experiment (Fig. VI.9.1) was undertaken so as to simulate the relative sampling of the array. Fig. VI.9.1a shows the 'transparent' medium in form of an epoxy box (v_p=2.6 km s^{-1}) and the embedded inhomogeneity in form of an aluminium cross (v_p=5.2 km s^{-1}). The size of the box is 80 • 50 • 50λ^3 (wavelengths), while the standard length and width of the individual arms in the cross are ~12λ and ~2λ respectively. The spacing between the source (diameter 12λ) and the cross is 30λ and the sensor grid area on the surface is 15λ • 15λ, Fig. VI.9.1b) gives the two sensor configurations used, namely, i) a rectangular grid with 2025 sensors with an interspacing of $\lambda/3$ and ii) a 132-sensor geometry similar to that of the NORSAR array. Fig. VI.9.1c is image reconstruction of the cross (outlined) at its correct depth location on the basis of the regular grid network with contributions from all 2025 sensors to each reconstructed point. Relative intensity scaling is used with contour levels at 1, 2, 4 & 8 dB. Fig. VI.9.1d shows the same as 1c except that contributions are restricted to those observational points being within a radius equal to the diameter of the first Fresnel zones. Notice that for 1c and 1d the relatively high intensities observed at the center of the cross stem from a non-plane source illumination. This was actually discovered when reconstructing data for a model without inhomogeneity. Fig. VI.9.1e is image reconstruction of the cross when the observational points were limited to a simulated NORSAR array configuration of 132 sensors which in turn were extrapolated to a grid of 25 • 25 sensors with an interspacing of 0.6λ. Also, as in the case of Fig. VI.9.1d, contributions to each reconstructed point were limited to a radius equal to the diameter of the first Fresnel zone. Fig. VI.9.1f displays relative intensity as a function of image reconstruction depth for both configurations of Fig. VI.9.1b. The strongest intensity is found at the proper depth location of

the cross and this coincides with a minimum distance from the center of the reconstruction axis. The intensity estimations for depth exceeding approx. 30λ reflects reconstructions of the source itself. The intensity maximum at the depth of the cross and the coinciding center axis minimum distance both imply that depth resolution should be comparable to or even better than that of 3-D time inversion. Thus, we find the results in Fig. VI.9.1 very encouraging, indicating that a satisfactory reconstruction of essential features of an embedded body seems feasible.

For testing the earth holography concept in practice, NORSAR P-wave recordings of 3 deep earthquakes at teleseismic distances (South of Honshu, Hindu Kush and Western Brazil) were subjected to analysis. The seismogram information extraction for the first 10 sec of P waves was tied to (spectral) amplitudes and phases of harmonic component at 1.8 Hz. Also, for image reconstruction purposes the earth's crust was given a thickness of 36 km and with an average P-velocity of 6.5 km/s, while the lithosphere was considered a half space with a P-velocity of 8.2 km/s. Composite results for all 3 events analyzed and for the depths 100 km, 148 km and 212 km, exhibiting the most pronounced scattering features are shown in Fig. VI.9.2. Different shading is used to identify the 3 events and their relative intensity scaling is also given. Numbers and following arrows indicate the angle of incident and azimuth for each event, correspondingly. The contours of the various shaded areas are 4 dB down from the individual event maxima which in turn are marked by black dots. In Fig. VI.9.2a we notice a good overlap between the intensity areas for the different events. This is taken to imply that heterogeneities at this depth are most uniformly seen by the 3 events. Fig. VI.9.2b which has weaker intensities as compared to Fig. VI.9.2a also exhibits less of an overlap between the respective event intensity areas. Similar comments apply to Fig. VI.9.2c. The consistency in location of the intensity areas I, II and III between figures a, b, and c are taken to imply a significant depth extent of the heterogeneous bodies in question. For areas IV, V, and VI, the anomalies are rather weak here and are seen most clearly by the Western Brazil event. For comparison the P-residual

inversion results in terms of relative velocity perturbations in per cent for their model A, depth interval 85-135 km, are displayed in Fig. VI.9.2b (Christoffersson and Husebye, 1979). The agreement between these two types of seismic results is considered good. For more detailed information we refer to the paper of Troitskiy et al (1981).

E.S. Husebye
P. Troitskiy, Inst. of Physics of the Earth, Moscow, USSR

References

Aki, K., A. Christoffersson and E.S. Husebye (1977): Determination of the three-dimensional seismic structure of the lithosphere, J. Geophys. Res., 82, 277-295.

Berteussen, K.-A., A. Christoffersson, E.S. Husebye and A. Dahle (1975): Wave scattering theory in analysis of P-wave anomalies observed at NORSAR and LASA, Geophys. J. R. astr. Soc., 42, 403-417.

Christoffersson, A. and E.S. Husebye (1979): On three-dimensional inversion of P wave time residuals: options for geological modeling, J. Geophys. Res., 84, 6168-6176.

Troitskiy, P., E.S. Husebye and A. Nikolaev (1981): Earth holography experiment - lithospheric studies based on the principles of holography. (Submitted to 'Nature').

Fig. VI.9.1

Ultrasonic experimental set-up and results. Figure a) shows the 'transparent' medium in form of an epoxy box (v_p=2.6 km s^{-1}) and the embedded inhomogeneity in form of an aluminium cross (v_p=5.2 km s^{-1}). The size of the box is 80 50 50 (wavelengths), while the standard length and width of the individual arms in the cross are ~ 12λ and ~ 2` respectively. The spacing between the source (diameter 12λ) and the cross is 30λ and the sensor grid area on the surface is 15λ • 15λ, Figure b) gives the two sensor configurations used, namely, i) a rectangular grid with 2025 sensors with an interspacing of λ/3 and ii) a 132-sensor geometry similar to that of the NORSAR array. Figure c) is image reconstruction of the cross (outlined) at its correct depth location on the basis of the regular grid network with contributions from all 2025 sensors to each reconstructed point. Relative intensity scaling is used with contour levels at 1, 2, 4 & 8 dB. Figure d) same as for c) except that contributions are restricted to those observational points being within a radius equal to the diameter of the first Fresnel zones. Notice that for c) and d) the relatively high intensities observed at the center of the cross stem from a non-plane source illumination. This was actually discovered when reconstructing data for a model without inhomogeneity. Figure e) is image reconstruction of the cross when the observational points were limited to a simulated NORSAR array configuration of 132 sensors which in turn were extrapolated grid of 25 • 25 sensors with an interspacing of 0.6λ. Also, as in case of Figure d) contributions to each reconstructed point were limited to a radius equal to the diameter of the first Fresnel zone. Figure f) displays relative intensity as a function of image reconstruction depth for both configuration of Figure b). The strongest intensity is found at the proper depth location of the cross and this coincides with a minimum distance from center of the reconstruction axis. The intensity estimations for depth exceeding approx. 30λ reflects reconstructions of the source itself. The intensity maximum at the depth of the cross and the coinciding center axis minimum distance both imply that depth resolution should be comparable to or even better than that of 3-D time inversion[4,5].

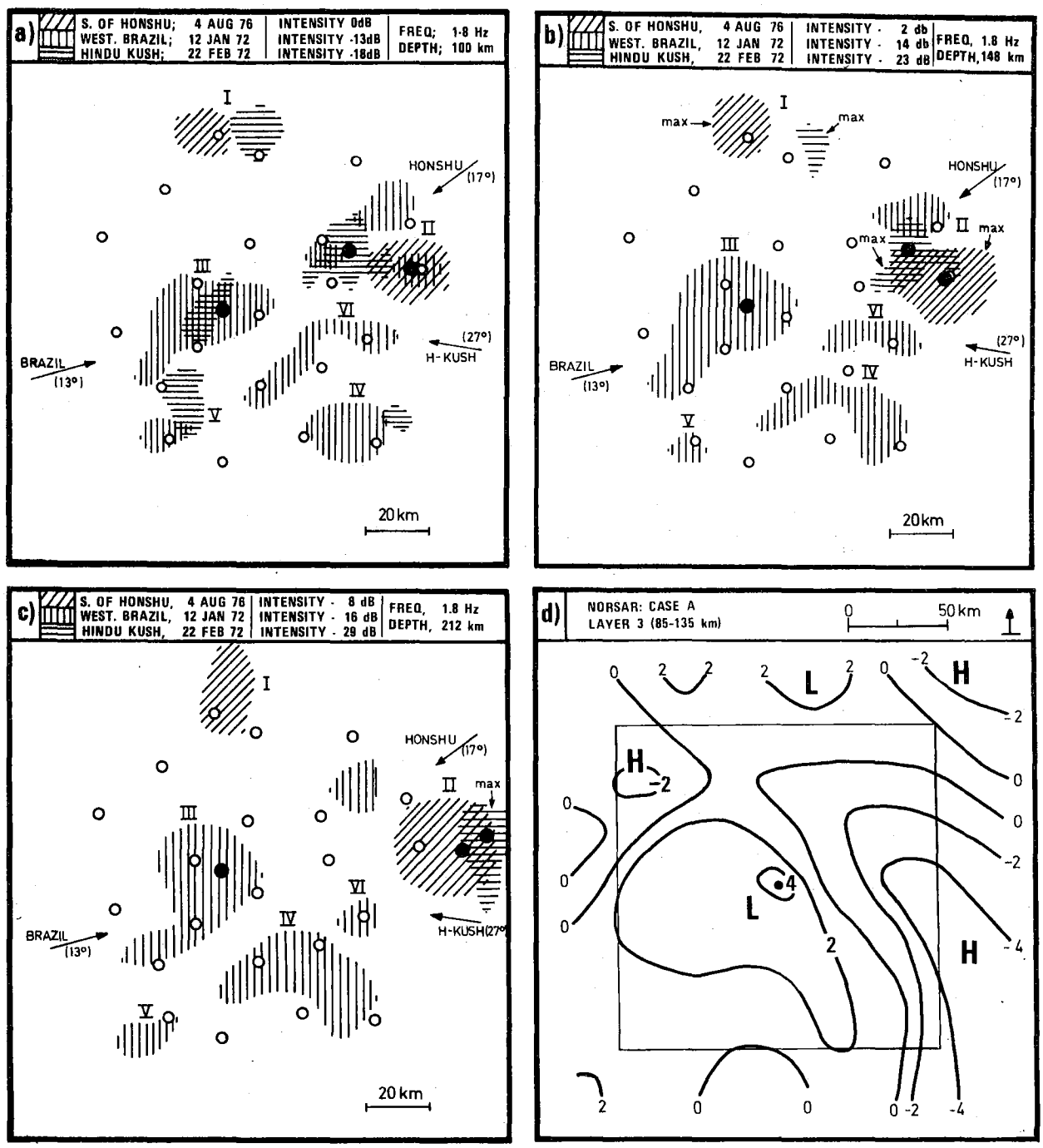
a)
S. OF HONSHU; 4 AUG 76
WEST. BRAZIL; 12 JAN 72
HINDU KUSH; 22 FEB 72
INTENSITY 0dB
INTENSITY -13dB
INTENSITY -18dB
FREQ; 1-8 Hz
DEPTH; 100 km
HONSHU (17°)
BRAZIL (13°)
(27°) H-KUSH
20 km
b)
S. OF HONSHU, 4 AUG 76
WEST. BRAZIL, 12 JAN 72
HINDU KUSH, 22 FEB 72
INTENSITY - 2 db
INTENSITY - 14 db
INTENSITY - 23 dB
FREQ, 1.8 Hz
DEPTH, 148 km
max
HONSHU (17°)
BRAZIL (13°)
(27°) H-KUSH
20km
c)
S. OF HONSHU, 4 AUG 76
WEST. BRAZIL, 12 JAN 72
HINDU KUSH, 22 FEB 72
INTENSITY - 8 dB
INTENSITY - 16 dB
INTENSITY - 29 dB
FREQ, 1.8 Hz
DEPTH, 212 km
HONSHU (17°)
BRAZIL (13°)
H-KUSH(27°)
20 km
d)
NORSAR: CASE A
LAYER 3 (85-135 km)
0 50km
L
H
-2
-4
2
0

Fig. VI.9.2

Fig. VI.9.2

Composite display of intensity maxima for the 3 depths 100, 148 and 212 km exhibiting the most pronounced scattering features. Different shading is used to identify the 3 events and their relative intensity scaling is also given. The contours of the various shaded areas are 4 dB down from the individual event maxima which in turn are marked by black dots. In figure a) we notice a good overlap between the intensity areas for the different events. This is taken to imply that heterogeneities at this depth are most uniformly seen by the 3 events. Figure b) which has weaker intensities as compared to figure a) also exhibits less of an overlap between the respective event intensity areas. Similar comments apply to figure c). The consistency in location of the intensity areas I, II and III between figures a), b) and c) are taken to imply a significant depth extent of the heterogeneous bodies in question. For comparison the P-residual inversion results[5] in terms of relative velocity pertubations in per cent for their model A, depth interval 85-135 km are displayed in figure b). The agreement between these two types of seismic results is considered good. Also notice that the time inversion results for the depth interval 185-235 km are essentially the same as those for the 85-135 km interval, implying decreasing resolution with increasing depth for this particular method.

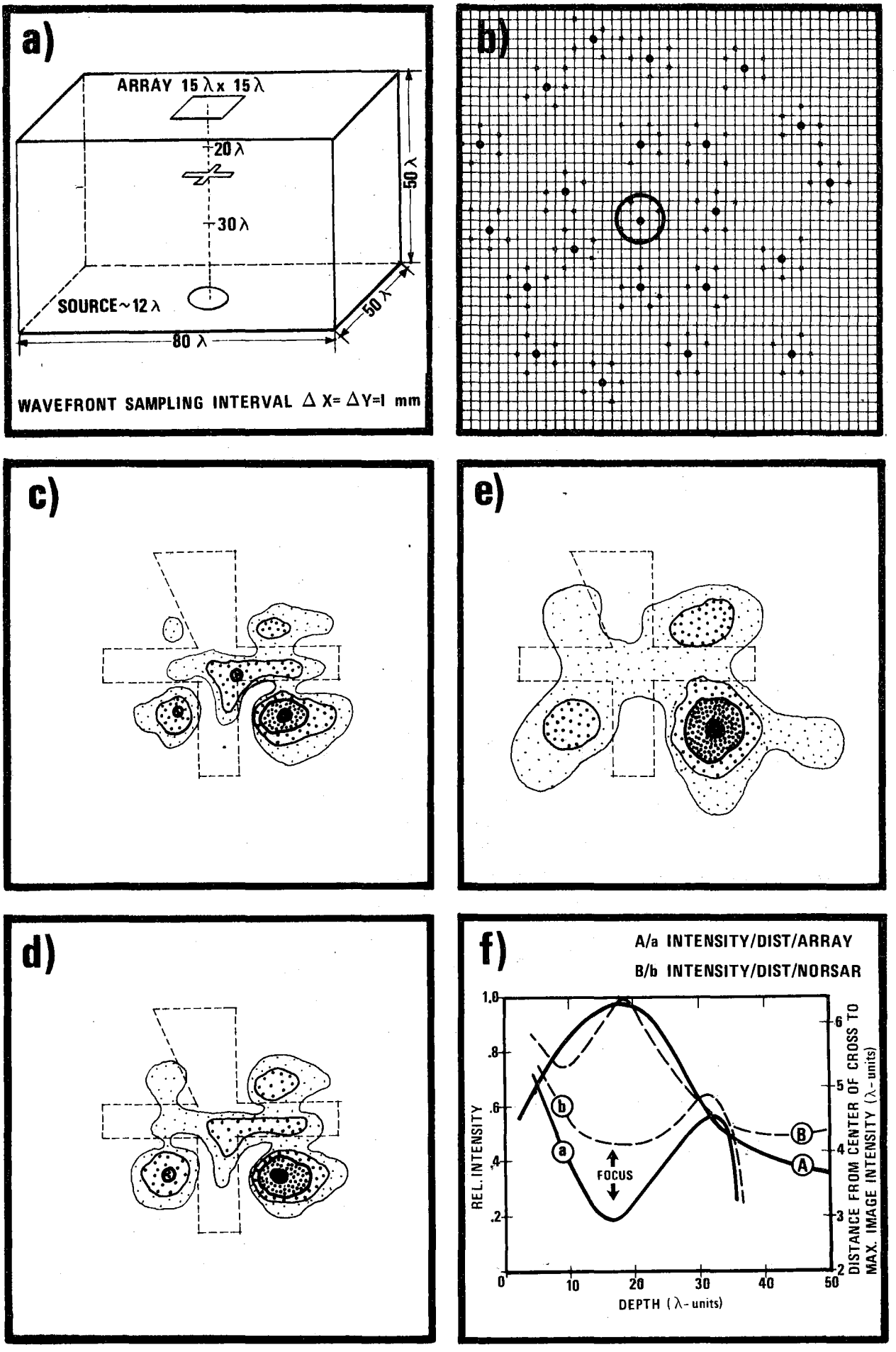
a)
ARRAY 15 λ x 15 λ
20 λ
30 λ
50 λ
SOURCE ~ 12 λ
50 λ
80 λ
WAVEFRONT SAMPLING INTERVAL Δ X = Δ Y = 1 mm
b)
c)
e)
d)
f)
A/a INTENSITY/DIST/ARRAY
B/b INTENSITY/DIST/NORSAR
REL. INTENSITY
1.0
.8
.6
.4
.2
0
10
20
30
40
50
DEPTH (λ-units)
FOCUS
a
b
A
B
DISTANCE FROM CENTER OF CROSS TO MAX. IMAGE INTENSITY (λ-units)
2
3
4
5
6

Fig. VI.9.1